PS Shortening Values in the Southern Fars Arch of the Zagros: Assessing Uncertainties by Structural and Gravity Sensitivity Analysis*

**Ralph Hinsch[1], Martin Vögele[1], Gholamreza Gharabeigli[2], Abbas Majidi[2],
Tam Lovett[1], Ali Asghar Julapour[2], Gabor Tari[1], and Walter Kosi[1]**

Search and Discovery Article #51668 (2020)**
Posted May 25, 2020

*Adapted from poster presentation given at 2019 AAPG Middle East Region, Geosciences Technology Workshop, 2nd Edition Structural Styles of the Middle East, Muscat, Oman, December 9-11, 2019

DOI:10.1306/51668Hinsch2020

[1]OMV Upstream, Exploration, Vienna, Austria (Ralph.Hinsch@omv.com)
[2]National Iranian Oil Company, Exploration Directorate, Vienna, Austria

Abstract

OMV Upstream and the National Iranian Oil Company conducted a joint geoscientific study in the southern Fars area from 11/2016 until 10/2018. The study area is located within the Simply Folded Belt of the Zagros, famous for its largescale whaleback folds and salt glaciers. Reflection seismic (on- and offshore), gravity, well and surface geology data were integrated to assess stratigraphic thicknesses/top basement morphology and to constrain reasonably balanced cross sections and shortening estimates. The modelling uncertainties are addressed and discussed based on thorough modelling parameter sensitivity studies. The amount of shortening in the balanced sections from the study varies from 8-15% whilst other published authors report values up to 25%. The main differences between the sections are the stratigraphic thicknesses used/depth to basement and the amount of internal/layer parallel shortening. Stratigraphic thicknesses were estimated from 3D gravity modelling, exploiting available depth-converted reflection seismic and velocity data, as well as log information from multiple offshore wells (used for Gardner co-efficient calibration). The resulting density model was subsequently used to quantify depth-to-basement uncertainties and later to structurally invert for the crystalline basement depth. This modelling exercise suggests that gravity inversion results are driven by density uncertainties in the thick Paleozoic strata and the basement rocks. Resulting uncertainties up to +/-3.5 km on top basement location can therefore be expected. An area balancing approach shows that lower shortening values (< 15%) can be achieved using high stratigraphic thicknesses (11-13 km) and a general mild dip of the decollement (0.5°) towards the North. High shortening values (> 20%) are required for thin stratigraphic thicknesses (9-11 km) and/or a high dip of the basement (1°) towards the North. The study results indicate an overall high uncertainty that needs to be considered for balanced sections in the Fars area and, consequently, reported shortening values might have a relatively high spread. Furthermore, based on the uncertainties in balancing alone, it is not possible to clearly define whether basement is actively involved in the deformation or not.

References Cited

Alavi, M., 2007, Structures of the Zagros fold-thrust belt in Iran: American Journal of Science, v. 307/9, p. 1064–1095.

Jahani, S., J.-P. Callot, J. Letouzey, and D. Frizon de Lamotte, 2009, The eastern termination of the Zagros Fold-and-Thrust Belt, Iran: structures, evolution, and relationships between salt plugs, folding, and faulting: Tectonics, v. 28, p. TC6004.

Jahani, S., J. Hassanpour, S. Mohammadi-Firouz, J. Letouzey, D. Frizon de Lamotte, S. A. Alavi, and B. Soleimany, 2017, Salt tectonics and tear faulting in the central part of the Zagros Fold-Thrust Belt, Iran: Marine and Petroleum Geology, v. 86, p. 426-446.

Judge, P.A., and R.W. Allmendinger, 2011, Assessing uncertainties in balanced cross sections: Journal of Structural Geology, v. 33/4, p. 458–467.

Konert, G., A. Afifi, S. Al-Hajri, and H. Droste, 2001, Paleozoic Stratigraphy and Hydrocarbon Habitat of the Arabian Plate: GeoArabia, v. 6/3.

Laske, G., G. Masters., Z. Ma, and M. Pasyanos, 2013, Update on CRUST1.0 - A 1-degree Global Model of Earth's Crust: Geophys. Res. Abstracts, v. 15, Abstract EGU2013-2658.

Molinaro, M., P. Leturmy, J.-C. Guezou, D. Frizon de Lamotte, and S.A. Eshraghi, 2005, The structure and kinematics of the south-eastern Zagros fold-thrust belt; Iran: from thin-skinned to thick-skinned tectonics: Tectonics, v. 24, p. Tc3007.

Motamedi, H., S. Sherkati, and M. Sepehr, 2012, Structural style variation and its impact on hydrocarbon traps in central Fars, Southern Zagros folded belt: Iran. J. Struct. Geol. v. 37, p. 124-133.

Nissen, E., J. Jackson, S. Jahani, and M. Tatar, 2014, Zagros “phantom earthquakes” reassessed - the interplay of seismicity and deep salt flow in the Simply Folded Belt? J. Geophys. Res. Solid Earth, v. 119/4, p. 3561-3583.

Nissen, E., M. Tatar, J.A. Jackson, and M.B. Allen, 2011, New views on earthquake faulting in the Zagros fold-and-thrust belt of Iran: Geoph. J. Int., v. 186/3, p. 928–944.

Parker, R.L., 1972, The Rapid Calculation of Potential Anomalies: J. Geophys. Res., v. 31, p. 447–455.

Sandwell, D.T., and W.H.F. Smith, 2009, Global marine gravity from retracked Geosat and ERS 1 altimetry: Ridge segmentation versus spreading rate: J. Geophys. Res., v. 114, p. B01411.

Talebian, M., and J.A. Jackson, 2004, A reappraisal of earthquake focal mechanisms and active shortening in the Zagros mountains of Iran: Geoph. J. Int., v. 156, p. 506–526.

AAPG | Geosciences Technology Workshops 2019

9-11 DECEMBER 2019
SUNDUS ROTANA
MUSCAT, OMAN

2ND EDITION
STRUCTURAL STYLES
OF THE MIDDLE EAST

Shortening values in the southern Fars arch of the Zagros: assessing uncertainties by structural and gravity sensitivity analysis

Ralph Hinsch[1], Martin Vögele[1], Gholamreza Gharabeigli[2], Abbas Majidi[2], Tam Lovett[1], Ali Asghar Julapour[2], Gabor Tari[1], Walter Kosi[1]

1.OMV Upstream, Exploration, Vienna, Austria, ralph.hinsch@omv.com 2.National Iranian Oil Company, Exploration Directorate, Tehran, Iran

Box 1 Introduction

1. Introduction

OMV Upstream and the National Iranian Oil Company conducted a joint geoscientific study from 11/2016 until 10/2018. The study area is located within the Simply Folded Belt of the Zagros (Fig. I1), an area with abundant past studies. We like to draw attention to the uncertainties still inherent in the interpreted data, from initial interpretations (e.g. of geophysical data) to balanced sections. For the latter, one important input is the knowledge of the stratigraphic thickness / depth to basement.

2. Setting

The Simply Folded Belt of the SE Fars region represents a fold belt of Cambrian to recent sediments of the Arabian Shield detached on the Hormuz evaporites (Figs. I1 - I3). Stratigraphic control in the study area is down to Triassic (outcrop) or Permian (wells). The undeformed stratigraphic thickness can be estimated close to the deformation front (see Fig. I1). Offshore a dense grid of 2D seismic lines is present (e.g. Fig. G1). Stratigraphic thicknesses estimates vary significantly (Tab. I1). Consequently, balanced sections in the area show different structural styles and have different shortening values (Fig. I2).

Relocated seismic events usually plot within the sediments (Talebian and Jackson 2004) but some microseismicity and earthquakes are located in the basement (Nissen et al. 2011, 2014). How much is the basement included in recent active deformation and contributes to the cross sectional area above the regional elevation?

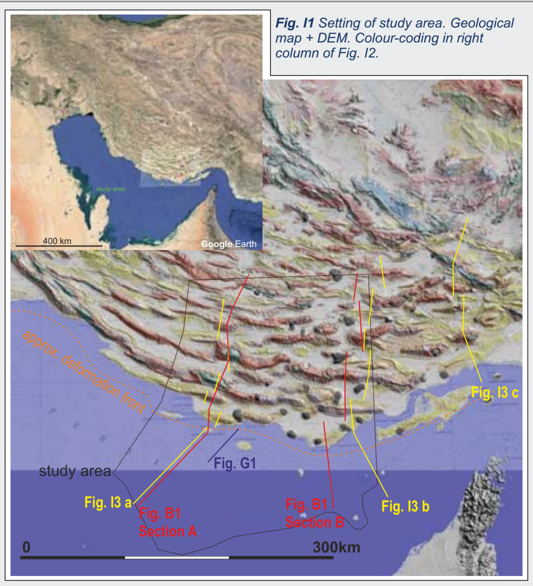

Fig. I1 Setting of study area. Geological map + DEM. Colour-coding in right column of Fig. I2.

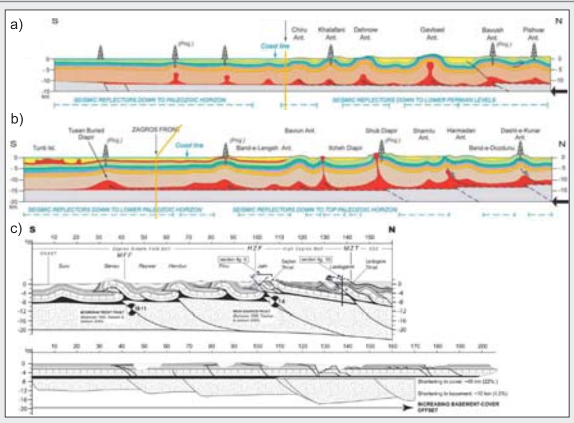

Fig. I2 Sections from literature
a) 12.7 km (9%; Jahani et al. 2009)
b) 10.5 km (6%, Jahani et al. 2009)
c) 45 km (22%) (Molinaro et al., 2005) or 25 km (20%) south of the HZF.

estimated stratigraphic thickness	source
6 km	Alavi 2007, Section F
8 km	Molinaro et al. 2005
12 km	Jahani et al. 2009
16 km	Jahani et al. 2017

Tab. I1: Estimated stratigraphic thicknesses (published sections) close to deformation front

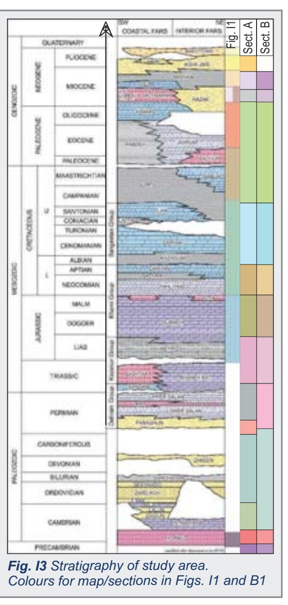

Fig. I3 Stratigraphy of study area. Colours for map/sections in Figs. I1 and B1

Overview:

In this study we use different data and methods to assess uncertainties.

Box 1 gives and introduction to the area and the problem

Box 2 uses geophysical data and methods to estimate the depth to basement and related uncertainties.

Box 3 uses geological balancing methods to estimate the shortening of sections and to assess the impact of input uncertainties on the shortening values and the potential contribution of the basement.

Box 2 Geophysics

1. Objective

Reflection seismic (on- and offshore), gravity, well and surface geology data were integrated into a consistent model to evaluate stratigraphic thicknesses/top basement depths and associated uncertainties. We use time domain seismic interpretation and depth conversion as well as inverse modelling of gravity data.

Data is well constrained by outcrops and by wells down to Permian levels.

2. Reflection seismic and time to depth conversion

The velocity model to Permian is constrained by seismic migration velocities and offshore wells. Constant velocities for Lower Paleozoic and Hormuz salt is used. Seismic data quality is reasonable down to Permian level. It is difficult to interpret the deeper Paleozoic and the Hormuz salt layers (see two possible interpretations in Fig. G1). The related depth uncertainties of the top salt interpretations (Fig. G1 and G4) in combination with velocity uncertainties may result in relative depth uncertainties to top basement of up to 4000 m (Fig. G2).

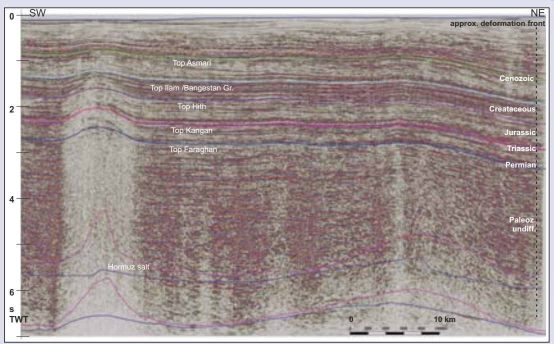

Fig. G1: 2D seismic line (off-shore). Well control down to blue horizon. Two tentative interpretations of Top and Base Hormuz salt are shown.

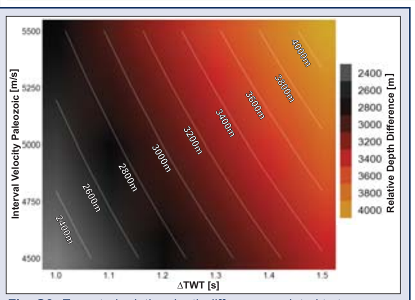

Fig. G2: Expected relative depth differences related to two plausible Hormuz salt interpretations and velocity uncertainties in the Paleozoic. Depending on the TWT difference of the picks and the interval velocity for the Paleozoic, relative depth uncertainties may become as large as 4000m

3. Density model building and input gravity inversion and input gravity data

Gardner co-efficients were calibrated for four zones down to Permian using selected key wells (Fig. G3). These co-efficients were subsequently used with the seismic velocity model to obtain a bulk density cube as basis for the gravity inversion.

The gravity data from NIOC was re-processed and harmonized, merged, and reduced to a single simple Bouguer anomaly grid corrected with 2.2g/cc.

The regional-residual gravity was calculated by removing the effect of a forward modelled gravity attraction of a model crust from the CRUST1.0 model (Laske et al., 2013; Fig. G3).

4. Gravity inversion and sensitivity studies

Depth-to-basement estimates from gravity data were obtained by inverting for the basement depth and iteratively minimising the misfit between observed and forward-calculated gravity response from the corresponding 3D density model (see Parker, 1972).

In order to quantify the modelling sensitivities, a simplified density model was built (Fig. G5) and used to calculate responses with varying parameters (Tab. G1).

Figure G6 depicts the resulting misfits in milligal between the reference gravity anomaly and the modelled scenarios. The corresponding resulting basement depth misfits are shown for scenarios a) – c) in Fig. G7.

Basement depths of the two geological models from Fig. G4 were inverted to minimise the misfit between observed and modelled gravity data.

The impact of velocity uncertainties in the Paleozoic is presented exemplarily in Fig. G8 using constant salt densities of 2.2 g/cc and basement densities of 3.0 g/cc.

5. Discussion and Conclusion *Geophysics*

Uncertainties from reflection seismic interpretation and time to depth conversion can result in basement depth uncertainties of more than 3000 m.

The gravity modelling exercise has demonstrated that depth-to-basement estimates from potential field data need to be interpreted with care. Modelling uncertainties are related to the inherent non-uniqueness of potential field data and the lack of data or insufficient data resolution for constraining the model. Both endmember models manage to approximate the residual measured gravity anomaly in the study area. However, the resulting absolute basement depth differs by approximately 3500 m. The morphology of the tentative top basement maps is in accordance with previous publications (e.g. Konert et al., 2001).

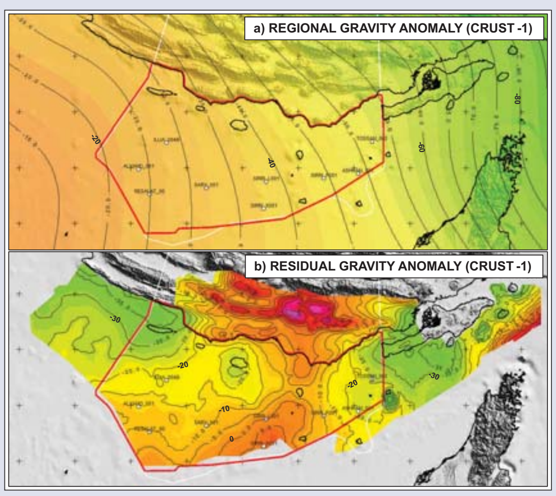

*Fig. G3: **a)** Forward-modelled regional gravity effect from the CRUST1.0 model and resulting residual gravity anomaly in miligal. **(b)** Resulting residual anomaly for 5 reprocessed surveys, (Bouguer anomaly grid corrected with a density of 2.2g/cc). Red: Outline of the 3D density model and selected key wells.*

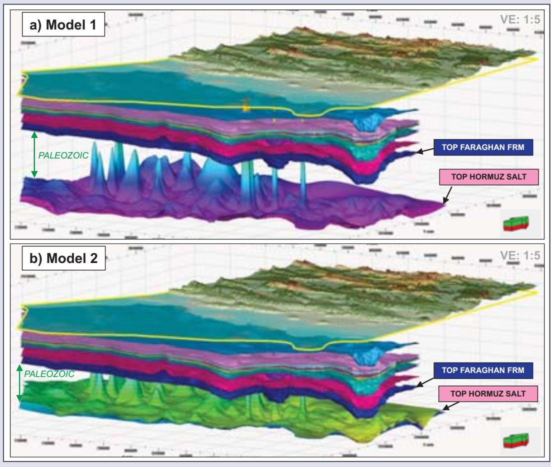

*Fig. G4: 3D depth surfaces for creating the input density models. The two models as in **a)** and **b)** differ mainly in the Hormuz salt depth, driven by the time pick and the average seismic velocity selected for the Paleozoic.*

Box 3 Balancing

1. Balanced sections

Two balanced and restored sections have been constructed in this study (Fig. B1).

Sect. A: The western section (after first year of the study) has less constraints on the deformation in the anticlines (less internal deformation features) and used a relatively high stratigraphic thickness at the deformation front (13875 m). Slight basement inversion has been assumed (average basement dip deformed: 0.9°, restored: 1°, restored Top Miocene Mishan is about horizontal). Pure line-length balancing of Top Mishan reveals 7.1% shortening, Tab. B1.

Sect. B The eastern section (in second 2 year of the study) has better seismic control and shows shortening structures inside anticlines. Stratigraphic thickness at the deformation front is 11575 m. Some minor inversion have been assumed as well. The pre-kinematic restored section has an average dip towards the hinterland of 0.46° (Top Miocene Mishan Fm.) and 0.6° at top basement level. Pure line-length balancing of Top Mishan reveals 13.5 % shortening, Tab. B1.

The line length shortening is close to a minimum estimate (especially in the western section), as there is little scope to have less line length in the deformed state. However, there could be additional internal shortening, which is not considered in the present sections.

The average plunge of the basement results from plunge from basin basement after rift/post-rift history + far field flexural response + reduction by basement shortening.

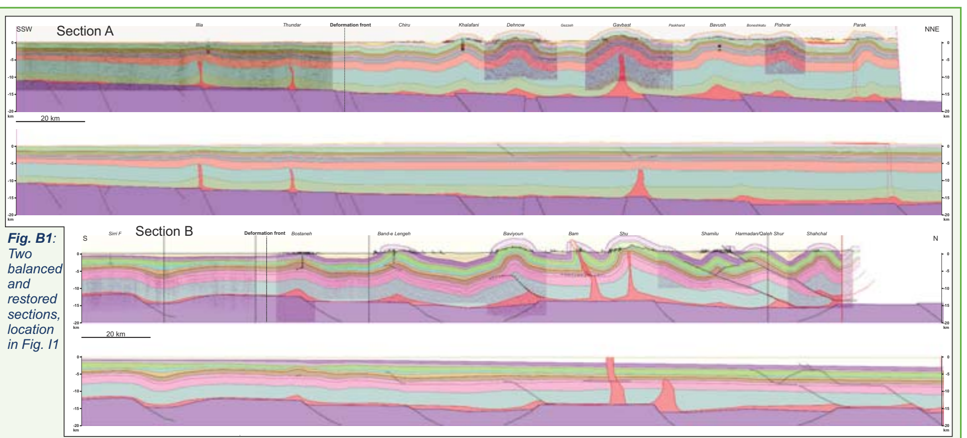

Fig. B1: Two balanced and restored sections, location in Fig. I1

	Strat. thickness @ def. front. [m]	Deformed Top Mishan Fm. [m]	Restored line length [m]	Shortening [m]	Shortening [%]
Section A	13873	159500	172500	13000	7.5
Section B	11575	220500	255000	34500	13.5

Tab. B1: Key values measured for section A + B

2. Area balancing

Area balancing is a kinematic independent approach which can be used as analytical tool to estimate uncertainties in shortening values (Judge and Allmendinger 2011).

Here, we use area balancing to estimate shortening values by changing some of the main uncertainties:

1. The stratigraphic thickness at the deformation front
2. The dip at the base of the sediments (thickness increase towards the hinterland or influence of basement involvement in the deformation)

We use slightly simplified versions of Section A + B as base cases. The area supporting the folded Miocene Mishan Fm. above basement (A1) in the deformed section needs to be the same when restored to sea level (A2). We split the area into geometrical sub-areas and measure the folded area above a certain datum (i.e. A1a above Y1a,) and the section length (X1). The other sub-areas (A1b, A1c) are geometrically calculated on variable parameters (i.e. dip of the basement [β], stratigraphic thickness [Y1a+Y1b]). The length of the restored section (X2) is iteratively calculated by minimizing the error of A1 to A2 until (A1a+A1b+A1c) = (A2a+A2b+A2c).

For both sections we use variable stratigraphic thicknesses (7000 - 15000 m). Additionally the dip of the basement in deformed and restored section is slightly varied:

β1 > β2 : it can be considered that the deformed section has some regional flexural component. Resulting shortening values are higher in comparison to a constant β.

β1 < β2 : can be considered as result of basement shortening. Thick-skinned reverse faults bring basement rocks above regional elevation and lowering the average basement dip. Consequently, less shortening is required in the sediments in comparison to a constant β.

The resulting shortening values are listed in Tab. B2.

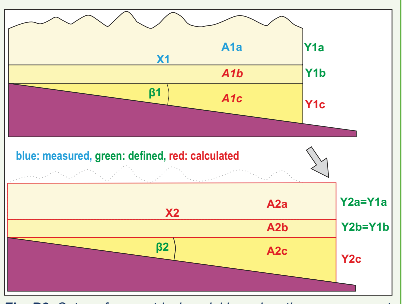

Fig. B2: Setup of geometrical model based on the measurement of the area A1 and the section length X1 from sections in Fig. B1

case	Strat. Thickness [m]	Basement dip ß1 [deg]	Basement dip ß2 [deg]	Shortening [m]	Shortening [%]
Section A simplified	13873	1	1.11	13000	7.5
constant low ß	7000	0.50	0.50	21977	12.1
	9000	0.50	0.50	17817	10.0
	11000	0.50	0.50	14974	8.6
	13000	0.50	0.50	12911	7.5
	15000	0.50	0.50	11345	6.6
constant ß	7000	1.00	1.00	17063	9.7
	9000	1.00	1.00	15648	8.9
	11000	1.00	1.00	13419	7.8
	13000	1.00	1.00	11742	6.9
	15000	1.00	1.00	10436	6.1
Increasing ß 0.25	7000	1.00	1.25	11292	6.6
	9000	1.00	1.25	10403	6.1
	11000	1.00	1.25	8987	5.3
	13000	1.00	1.25	7908	4.7
	15000	1.00	1.25	7060	4.2
Increasing ß 0.5	7000	1.00	1.50	6158	3.7
decreasing ß 0.5	7000	1.00	0.50	31233	16.4
	9000	1.00	0.50	28298	15.1
	11000	1.00	0.50	23813	13.0
	13000	1.00	0.50	20547	11.4
	15000	1.00	0.50	18066	10.2
decreasing ß 0.75	7000	1.00	0.25	40200	20.1
	9000	1.00	0.25	36120	18.5
	11000	1.00	0.25	30019	15.8
	13000	1.00	0.25	25674	13.9
	15000	1.00	0.25	22424	12.3
Section B simplified	11575	1	0.47	34137	13.4
constant low ß	7000	0.5	0.50	25502	10.4
	9000	0.5	0.50	20919	8.7
	11000	0.5	0.50	17724	7.4
	13000	0.5	0.50	15372	6.5
	15000	0.5	0.50	13570	5.8
constant ß	7000	1	1.00	19174	8.0
	9000	1	1.00	17718	7.4
	11000	1	1.00	15378	6.5
	13000	1	1.00	15372	6.5
	15000	1	1.00	12156	5.2
Increasing ß 0.25	7000	1	1.25	10395	4.5
decreasing ß 0.5	7000	1	0.50	43823	16.6
	9000	1	0.50	39938	15.3
	11000	1	0.50	33910	13.3
	13000	1	0.50	29449	11.8
	15000	1	0.50	26019	10.5
decreasing ß 0.75	7000	1	0.25	60455	21.5
	9000	1	0.25	54530	19.8
	11000	1	0.25	45578	17.1
	13000	1	0.25	39135	15.1
	15000	1	0.25	34281	13.4
decreasing ß 0.9	7000	1	0.10	72642	24.7
	9000	1	0.10	64992	22.7
	11000	1	0.10	53678	19.6
	13000	1	0.10	45709	17.1
	15000	1	0.10	39796	15.3

Tab. B2: Calculated shortening results from area balancing for variable stratigraphic thickness at deformation front and variable basement dips for section A and B.
Red numbers are above 150% or below 80% of the calculated shortening value for the original section. These values might be considered unrealistic with the given known constraints (i.e. surface geological map, dips, etc.)

3. Discussion and conclusions *Balancing*

The results of the area balancing models are in Tab. B2. A thinner sedimentary cover needs higher shortening values to support the observed structural elevations of the anticlines than a thick cover. Changing the basement dip has the same effect on shortening – because it is increasing or decreasing the assumed stratigraphic thickness north of the deformation front.

Consequently, an observed cross section area can be achieved by varying amounts of shortening and/or contribution from basement.

It can be doubted that the stratigraphic thicknesses used in published balanced sections in the Fars region vary from 6 - 16 km. Consequently, shortening values are likely not varying from 6-20 % (using % as indicator of structural style for sections of different length and position).

It would be helpful if all balanced sections would be published along with a discussion on the certainty level of all used input parameters and a reasonable upper and lower shortening value. Understanding the uncertainties strongly affect the discussion on how much the basement is actually shortened in the Simply Folded Belt.

We conclude that geological shortening from balancing has a high uncertainty in the Fars area. Section balancing is not sufficient to define whether basement is (significantly) shortened or not. To solve this question other observations and methods should be combined into a consistent and plausible model.

Acknowledgements

We thank OMV and NIOC to be able to present some study results which are of possible interest to the scientific community.

We thank all participants of the study for their valuable input. B. Bretis is thanked for the redrafting of the stratigraphic column.

References

Alavi, M., 2007. Structures of the Zagros fold-belt in Iran. American Journal of Science 307 (9), 1064–1095

Jahani, S., Callot, J.-P., Letouzey, J., Frizon de Lamotte, D., 2009. The eastern termination of the Zagros Fold-and-Thrust Belt, Iran: structures, evolution, and relationships between salt plugs, folding, and faulting. Tectonics 28, TC6004.

Jahani, S., J. Hassanpour, S. Mohammadi-Firouz, J. Letouzey, D. Frizon de Lamotte, S. A. Alavi, B. Soleimany, 2017, Salt tectonics and tear faulting in the central part of the Zagros Fold-Thrust Belt, Iran, Marine and Petroleum Geology 86 (2017) 426-446

Judge, P. A., and R. W. Allmendinger, 2011, Assessing uncertainties in balanced cross sections: Journal of Structural Geology, v. 33, no. 4, p. 458–467

Konert, G., Afifi, A., Al-Hajri, S., and Droste, H. (2001): Paleozoic Stratigraphy and Hydrocarbon Habitat of the Arabian Plate, GeoArabia, Vol. 6(3)

Laske, G., Masters., G., Ma, Z. and Pasyanos, M. (2013): Update on CRUST1.0 - A 1-degree Global Model of Earth's Crust. Geophys. Res. Abstracts, 15, Abstract EGU2013-2658

Molinaro, M., Leturmy, P., Guezou, J.-C., Frizon de Lamotte, D., Eshraghi, S.A., 2005. The structure and kinematics of the south-eastern Zagros fold-thrust belt; Iran: from thin-skinned to thick-skinned tectonics. Tectonics 24, Tc3007

Motamedi, H., Sherkati, S., Sepehr, M., 2012. Structural style variation and its impact on hydrocarbon traps in central Fars, Southern Zagros folded belt. Iran. J. Struct. Geol. 37, 124-133

Nissen, E., Jackson, J., Jahani, S., Tatar, M., 2014. Zagros "phantom earthquakes" reassessed - the interplay of seismicity and deep salt flow in the Simply Folded Belt? J. Geophys. Res. Solid Earth 119 (4), 3561-3583

Nissen, E., Tatar, M., Jackson, J.A., Allen, M.B., 2011. New views on earthquake faulting in the Zagros fold-and-thrust belt of Iran. Geoph. J. Int. 186 (3), 928–944

Parker, R. L. (1972): The Rapid Calculation of Potential Anomalies. J. Geophys. Res., 31, pp.447 – 455.

Sandwell, D. T., and Smith, W. H. F. (2009): Global marine gravity from retracked Geosat and ERS 1 altimetry: Ridge segmentation versus spreading rate. J. Geophys. Res., 114, B01411,

Talebian, M., Jackson, J.A., 2004. A reappraisal of earthquake focal mechanisms and active shortening in the Zagros mountains of Iran. Geoph. J. Int. 156, 506–526.

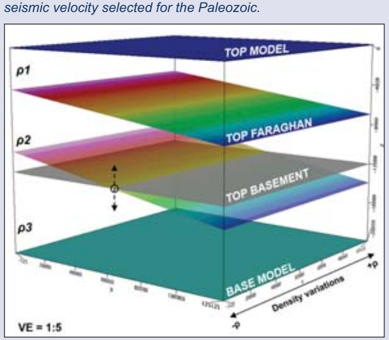

Fig. G5: Simplified three-layered model for testing basement depth uncertainties related to density variations and basement morphology. X-direction: layers dip (thickness), Y-direction = density variations. Parameters for scenarios are in Tab G1.

Scenario	Average Densities post Faraghan ρ1	Depth Top Faraghan	Average Densities Paleozoic ρ2	Depth Top Basement	Average Densities Basement ρ3
reference	2.55g/cc	4000 – 7000m	2.55g/cc	12000m	2.76g/cc
a)	**2.55g/cc +/- 2.5%**	4000 – 7000m	2.55g/cc	12000m	2.76g/cc
b)	2.55g/cc	4000 – 7000m	**2.55g/cc +/- 2.5%**	12000m	2.76g/cc
c)	2.55g/cc	4000 – 7000m	2.55g/cc	12000m	**2.67 – 2.85 g/cc**
d)	2.55g/cc	4000 – 7000m	2.55g/cc	**10000-14000m**	2.67 g/cc

Tab. G1: Model parameters for the reference case and the testing scenarios a) – d). Altered parameters are highlighted

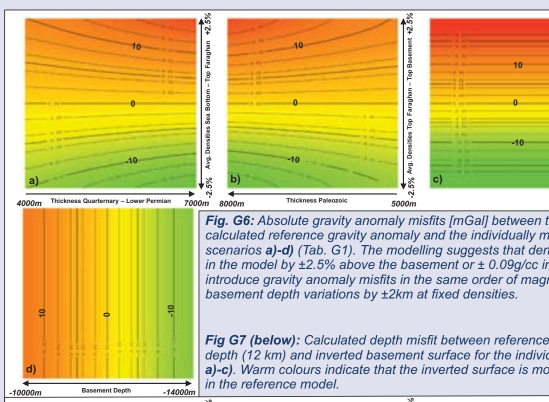

*Fig. G6: Absolute gravity anomaly misfits [mGal] between the forward calculated reference gravity anomaly and the individually modelled scenarios **a)-d)** (Tab. G1). The modelling suggests that density variations in the model by ±2.5% above the basement or ± 0.09g/cc in the basement introduce gravity anomaly misfits in the same order of magnitude as basement depth variations by ±2km at fixed densities.*

Fig G7 (below): *Calculated depth misfit between reference basement depth (12 km) and inverted basement surface for the individual scenarios **a)-c)**. Warm colours indicate that the inverted surface is more shallow than in the reference model.*

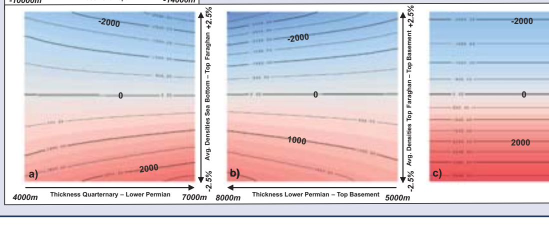

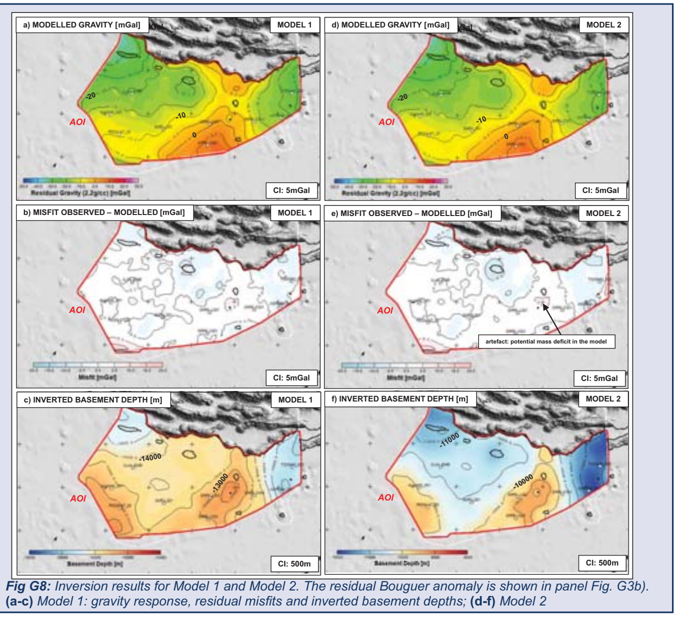

*Fig G8: Inversion results for Model 1 and Model 2. The residual Bouguer anomaly is shown in panel Fig. G3b). **(a-c)** Model 1: gravity response, residual misfits and inverted basement depths; **(d-f)** Model 2*